# Multiband Optical Switch Technology

**Takashi Goh[1], Keita Yamaguchi[2], and Ai Yanagihara[2]**
*1: NTT Electronics Corporation; 6700-2 To, Naka-shi, Ibaraki, 311–0122, Japan*
*2: NTT Device Innovation Center, NTT Corporation; 3-1 Morinosato Wakamiya, Atsugi, Kanagawa, 243–0198, Japan*
*takashi.goh.de@ntt-el.com*

**Abstract:** We developed a multiband switch element using a Mach-Zehnder interferometer with π shift utilizing wide and narrow waveguides for large fabrication tolerance. The fabricated 8×8 matrix switch using the element exhibited switch extinction ratios of more than 47 dB in wavelength from 1260 to 1675 nm. The average insertion loss was 1.8 dB including fiber coupling losses. © 2022 The Author(s)

## 1. Introduction

Optical switches are an indispensable device for flexible operation in the optical network systems used not only in traditional communication networks such as ROADM systems but also data center networks. Among the various types of optical switches, those using waveguide optics have attracted interest thanks to their excellent integration properties, stability, and mass productivity compared with those using free-space optics. Integrated optical switches such as multicast switches (MCSs) are widely used in practical communication systems [1].

The recent increases in traffic demands require multiband operations in the CL-band (1530–1625 nm) and higher. The operation wavelength range of conventional switches using waveguide optics is limited to a single band in practical scenarios because these switches use a Mach-Zehnder interferometer (MZI) with an optical path difference of half a wavelength. Although this wavelength range can deal with CL-band operation by using different optical path length differences in the MZI [2],[3], there are difficulties with operations in a wider wavelength range. While several designs have been proposed to increase the operating range of the switch [4],[5], one design has three times the number of phase shifters and the other uses two-stage lattice couplers, both of which make the configuration more complicated. In this paper, we propose a novel switch element for multiband operation with a simpler configuration along with a broadband 8×8 matrix switch using the element [6].

## 2. Broadband Switch Design

Figure 1 shows the configurations of (a) the proposed broadband switch element and (b) the conventional element. The basic configuration of both elements contains an MZI that consists of two cascade optical couplers with two waveguide arms and a thermo-optic phase shifter on one arm. In order to make the phase difference between the arm waveguides π when the phase shifter is in the off state, the conventional element has a waveguide length difference ΔL' of half the wavelength between the arm waveguides, while the proposed broadband switch element has a unique combination of wide and narrow waveguides in the arm waveguides in addition to ΔL.

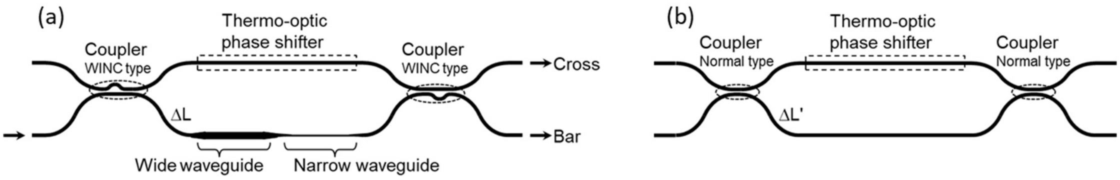


Fig. 1. Switch configurations of (a) proposed broadband switch element and (b) conventional switch element.

The arm phase difference Δϕ of the broadband switch element is expressed as

$$\Delta\phi = 2\pi\frac{n\cdot\Delta L+\Delta n_{wide}\cdot L_{wide}+\Delta n_{narrow}\cdot L_{narrow}}{\lambda}, \qquad (1)$$

where n is the equivalent refractive index of the normal waveguide, $\Delta n_{wide}$ and $\Delta n_{narrow}$ are the difference of the equivalent refractive index of the wide waveguide and narrow waveguide with respect to the normal waveguide, and $L_{wide}$ and $L_{narrow}$ are the length of the wide and narrow waveguides, respectively. The wavelength dependence of n can be approximated by the linear function of wavelength λ: $n(\lambda) \cong a\cdot\lambda + b$, where a and b are a function of the waveguide width. Thus, $\Delta n_{wide}$ and $\Delta n_{narrow}$ can also be expressed as the linear function of wavelength: $\Delta n'_{wide} \cong$

$a'_{wide} \cdot \lambda + b'_{wide}$, and as $\Delta n'_{narrow} \cong a'_{narrow} \cdot \lambda + b'_{narrow}$, where a'$_{wide}$, b'$_{wide}$, a'$_{narrow}$, and b'$_{narrow}$ are a function of the waveguide width, and Eq. 1 becomes

$$\Delta\phi = 2\pi\left\{a \cdot \Delta L + a_{wide} \cdot L_{wide} + a_{narrow} \cdot L_{narrow} + \frac{b' \cdot \Delta L + b'_{wide} \cdot L_{wide} + b'_{narrow} \cdot L_{narrow}}{\lambda}\right\}. \quad (2)$$

Therefore, by selecting ΔL, $L_{wide}$, and $L_{narrow}$ to satisfy $a' \cdot \Delta L + a_{wide} \cdot L_{wide} + a_{narrow} \cdot L_{narrow} = 0.5$ and $b' \cdot \Delta L + b'_{wide} \cdot L_{wide} + b'_{narrow} \cdot L_{narrow} = 0$, the Δϕ can be set to π over a wide wavelength range.

However, Δϕ tends to change significantly when the waveguide width shifts δW over the entire switch element due to fabrication process errors. This Δϕ change is caused by different amounts of variation in the equivalent refractive index n to the waveguide width shift δW when the designed waveguide width W is different. If the waveguide width shifts δW over the entire switch element, the variation in n of the wide or narrow waveguide in one arm is different from that on a normal waveguide in the other arm; in other words, the derivative of $\Delta n_{wide}$ or $\Delta n_{narrow}$ versus δW is not zero. To mitigate this Δϕ change, we choose an appropriate length ratio of $L_{wide}$ and $L_{narrow}$. First, we use the following equation to define the average value of the equivalent refractive indices of the wide and narrow waveguides, as

$$n_{avg} = \frac{L_{wide} \cdot n_{wide} + L_{narrow} \cdot n_{narrow}}{L_{wide} + L_{narrow}}, \quad (3)$$

where $n_{wide}$ and $n_{narrow}$ are the equivalent refractive index of the wide and narrow waveguide. With Eq. 3, Eq. 1 becomes

$$\Delta\phi = 2\pi \frac{n \cdot \Delta L + \Delta n_{avg} \cdot (L_{wide} + L_{narrow})}{\lambda}, \quad (4)$$

where $\Delta n_{avg}$ is

$$\Delta n_{avg} = n_{avg} - n = \frac{L_{wide} \cdot \Delta n_{wide} + L_{narrow} \cdot \Delta n_{narrow}}{L_{wide} + L_{narrow}}. \quad (5)$$

Since the derivative of $\Delta n_{wide}$ versus δW is negative, and the derivative of $\Delta n_{narrow}$ versus δW is positive, when we select the appropriate length ratio of $L_{wide}$ and $L_{narrow}$, the derivative of $\Delta n_{avg}$ versus δW becomes zero.

The type of optical coupler used in the switch element does not affect the switch extinction ratio, but only the loss characteristics. We use wavelength insensitive couplers (WINCs) in the proposed wideband switch element to obtain low insertion loss characteristics over a wide wavelength range.

## 3. Fabricated All-Band 8×8 Matrix Switch

We applied the broadband switch design described in the previous section to an 8x8 matrix switch. Figure 2(a) shows the 8×8 matrix switch configuration, which features path-independent insertion loss topologies. Figure 2(b) shows the double-gate switch unit as cross-point switch of the matrix switch. The double-gate switch unit consists of two switch elements to obtain a high extinction ratio. The matrix arrangement is almost the same as a conventional arrangement [2]. Specifically, we fabricated the 8×8 matrix using silica-PLC technology with the waveguide of the refractive index difference of about 2%, which enables a minimum bending radius of 1 mm. The widths of normal, wide, and narrow waveguides are 5, 9, and 3.5 μm, respectively. The design parameters of ΔL = 0.2836 μm, $L_{wide}$ = 542 μm, and $L_{narrow}$ = 397 μm are used in the broadband switch design. The chip size of the matrix switch is 7.6 × 80 mm. We also fabricated an 8×8 matrix switch with a conventional switch design for comparison.

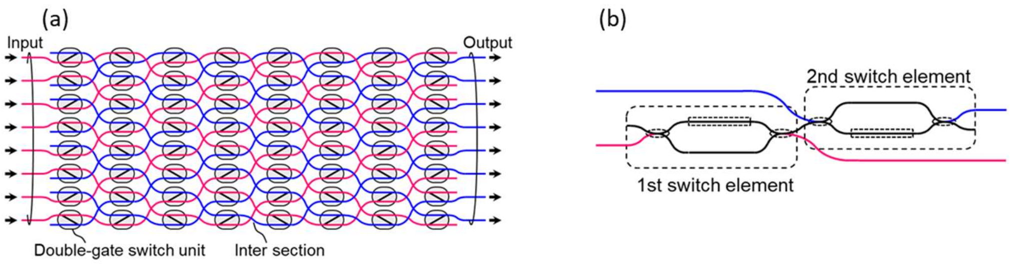


Fig. 2. Configuration of 8×8 matrix switch. (a) Matrix switch arrangement. (b) Double-gate switch unit.

Figure 3(a) shows the measured transmittance spectra of all 64 paths of the fabricated 8×8 matrix switch with the broadband switch design in the ON state and OFF state. An extremely flat response was successfully obtained in the entire operation wavelength range of the standard single-mode fiber. ON/OFF switch extinction ratios of more than 47 dB were achieved in the wavelength range of 1260 to 1675 nm. The average insertion loss was 1.8 dB including fiber coupling losses. In contrast, with the matrix switch of conventional switch design, the wavelength range with the high extinction ratio of more than 47 dB is limited to around the single C-band region, as shown in Fig. 3(b).

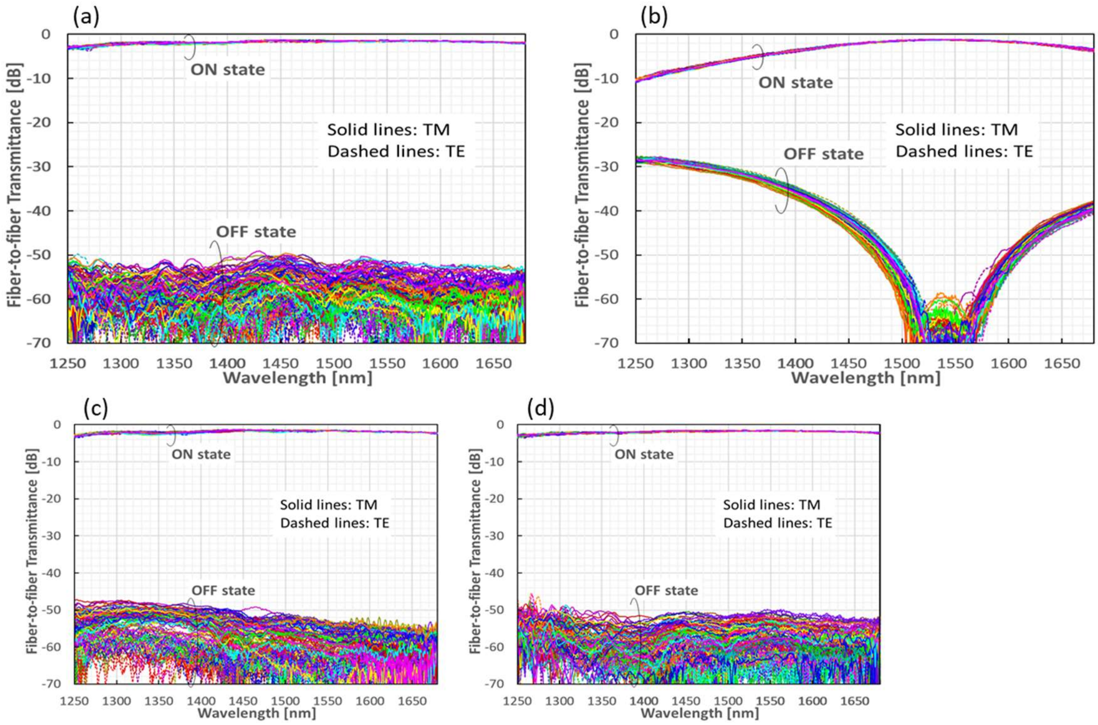


Fig. 3. Transmittance spectra of fabricated matrix switch: (a) broadband design, (b) conventional design, and (c) and (d) broadband design with the different exposure time in photo process of waveguides.

We also fabricated broadband 8×8 matrix switches with waveguide widths different from the design values by changing the exposure time in the photo process of waveguides using the same photo mask in order to determine the fabrication tolerance. Figure 3(c) and (d) shows the measured transmittance spectra of the fabricated broadband 8×8 matrix switches with 0.2 μm narrower and 0.1 μm wider waveguide widths than that of the matrix switch using normal exposure time, respectively. Almost no degradation of the insertion losses or switch extinction ratios was observed, confirming that the proposed broadband design has a large fabrication tolerance of more than 0.3 μm.

## 4. Conclusion

We developed a broadband switch element and demonstrated a broadband 8×8 matrix switch using the proposed element. The fabricated matrix switch exhibited excellent broadband characteristics that cover the entire wavelength range of a standard single-mode fiber for a communication system with a large fabrication tolerance. Our broadband design can be readily applied to other integrated switches such as MCS, and also applied to switches based on other material systems such as silicon, InP, and polymers, since it is a simple method of changing the waveguide width.

## References

[1] T. Watanabe et al., "Compact PLC-based Transponder Aggregator for Colorless and Directionless ROADM," in Proc. OFC/NEOEC 2011, OTuD3.
[2] T. Goh et al., "High Extinction Ratio and Low-Loss Silica-Based 8×8 Strictly Non-blocking Thermo-optic Matrix Switch," J. Lightwave Technol. 17(7), 1192–1199 (1999).
[3] S. Yamamoto et al., "First demonstration of a C+L band CDC-ROADM with a simple node configuration using multiband switching devices," Opt. Express **29**(22), 36353–36365 (2021).
[4] T. Kitoh et al., "Novel Broadband Optical Switch Using Silica-Based Planar Lightwave Circuit," IEEE Photon. Technol. Lett. **4**(7), 735–737 (1992)
[5] T. Watanabe et al., "Silica-based PLC 1×N Switch for All Wavelength Bands," in Proc. OFC 2014, Th1I.5.
[6] T. Goh et al., "All Wavelength Band 8×8 Optical Matrix Switch using Silica-Based Planar Lightwave Circuit Technology with Large Fabrication Tolerance," J. Lightwave Technol., to be submitted.